Journal of Hazardous Materials 179 (2010) 400–408

Contents lists available at ScienceDirect

Journal of Hazardous Materials

journal homepage: www.elsevier.com/locate/jhazmat

Effect of particle size in a limestone–hydrochloric acid reaction system

Bo Sun [a,c], Qulan Zhou [b,*], Xi Chen [c,d,e,*], Tongmo Xu [b], Shien Hui [b]

[a] Department of Power Machinery and Engineering, Shanghai Jiaotong University, Shanghai 200240, China
[b] The State Key Laboratory of Power Engineering Multiphase Flow, Xi'an Jiaotong University, Xi'an 710049, China
[c] Department of Earth and Environmental Engineering, Columbia University, New York, NY 10027, USA
[d] School of Aerospace, Xi'an Jiaotong University, Xi'an 710049, China
[e] Department of Civil & Environmental Engineering, Hanyang University, Seoul, 133-791, Korea

ARTICLE INFO

Article history:
Received 27 August 2009
Received in revised form
30 December 2009
Accepted 5 March 2010
Available online 11 March 2010

Keywords:
Limestone dissolution
Experiment
Particle

ABSTRACT

Experimental characterization of the wet flue gas desulfurization process is carried out using a model limestone–hydrochloric acid reaction system, with in-situ measurement of the dissolution rate and particle size distribution. The limestone source, initial particle size distribution, working temperature and pH value are varied in large ranges. The dissolution rate is found to be higher when the average particle size is smaller, the temperature is higher, or the pH is lower. An empirical equation is established to correlate the dissolution rate with the particle size and working conditions, which agrees well with measurements. The results may be useful for providing insights to improve the efficiency of the wet flue gas desulfurization process, as well as other solid particle–liquid solution reactions.

1. Introduction

The wet flue gas desulfurization (WFGD) [1–4] process is the most frequently used approach for environmental protection in thermal power plants, where the main component is the scrubbing process of wet type limestone. During this process, SO_2 from the flue gas is absorbed by the limestone slurry. The main content in the slurry is limestone particles ($CaCO_3$), which could dissolve and react with the dissolved SO_2 and O_2 to produce $CaSO_4{\cdot}2H_2O$. One of the most important characterizations [5] of the WFGD process is to accurately evaluate the dissolution rate of limestone; a challenge is that the size distribution of the limestone particle changes significantly during the reaction process – in order to better understand the working mechanisms of WFGD and optimize the process, in-situ characterization of the dissolution rate and particle size distribution is desired. On the other hand, note that the reaction between solid particles and liquid solution is very commonly encountered in nature and other engineering processes, an improved fundamental understanding of the critical factors affecting the reaction between limestone particles and acid solutions could also contribute to the fundamental discipline of liquid–solid flow.

Some previous studies of limestone dissolution have been carried out [6–13]. Several earlier works focused on the basic kinetics of calcite/limestone dissolution under typical conditions of WFGD [14–20], including the effects of pH value of liquid, limestone type, and particle size. An empirical relationship between pH, temperature, SO_2 partial pressure, and solution composition was developed by Chan and Rochelle [21], and verified by other studies [22,23]. Ukawa et al. [24] reported experimental results for the dissolution of limestone samples with different compositions and particle size distributions, which were in good agreement with a model based on the mass transfer mechanism. Ahlbeck et al. [25,26] measured the reactivity of limestone/lime absorbents by means of neutralization with a strong acid; however the effect of temperature was not considered in their investigation. Shih and Lin [27] studied the dissolution characteristics of limestone from six sources by using the pH-stat method in a stirred tank, however the adhered fine particles of the limestone samples must be washed away using ethanol, which was a complicated experimental step. Note that in almost all previous studies, the measurement was based on sequential/stepwise approach and to the best of authors' knowledge, in-situ characterization of the particle distribution profile and dissolution rate is still lacking – this is critical because the industrial desulfurization system is a continuous reactor and thus the process of dissolution cannot be interrupted.

In the present fundamental experimental study, we focus on the effect of microscopic size distribution of particles during the process of dissolution reaction, by employing a model system of limestone particles dissolution in acid. For different dissolution reactions with strong acid, the source of limestone, as well as the pH environment and temperature, are varied in large ranges to explore their influences. During a given experiment, the source of limestone, pH, and temperature are fixed at desired values, and the

* Corresponding authors.
E-mail addresses: qlzhou@mail.xjtu.edu.cn (Q. Zhou), xichen@columbia.edu (X. Chen).

0304-3894/$ – see front matter © 2010 Elsevier B.V. All rights reserved.
doi:10.1016/j.jhazmat.2010.03.018

Table 1
Contents of limestone.

Habitat	Contents					
	CaO (%)	MgO (%)	Al_2O_3 (%)	Fe_2O_3 (%)	Undissolved substance (%)	Bulk (kg/m^3)
Liquan limestone	52.76	0.00057	0.08064	0.3344	2.19	715.9
Tanyu limestone	51.91	3.03	0.08	0.24	3.88	649.8
Jiaochang limestone	53.59	1.92	0.08	0.24	3.98	646.3
Xinjiang limestone	50.22	0.91	1.71	1.08	4.52	663.2

Table 2
Average grain diameter of each sample.

Samples	Sample 1-1	Sample 1-2	Sample 1-3	Sample 1-4
Average grain diameter/μm	12.16	19.29	30.65	40.58
Samples	Sample 2-1	Sample 2-2	Sample 2-3	Sample 2-4
Average grain diameter/μm	12.58	18.99	21.21	39.23
Samples	Sample 3-1	Sample 3-2	Sample 3-3	Sample 3-4
Average grain diameter/μm	10.72	13.60	18.19	35.63
Samples	Sample 4-1	Sample 4-2	Sample 4-3	Sample 4-4
Average grain diameter/μm	11.09	16.81	27.69	34.32

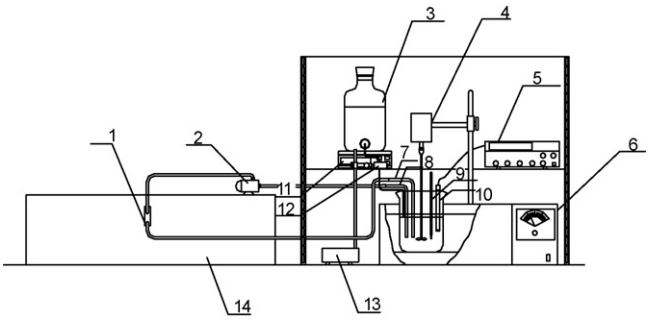

Fig. 1. Schematic of experimental setup.

measurements of the dissolution rate and particle size distribution are carried out in-situ. An empirical equation is proposed based on the fitting of experimental data, which could guide the dissolution process in practice.

2. Experimental procedure

2.1. Experimental fixture

Fig. 1 shows the experimental fixture. A model strong acid is used in the dissolution experiment to replace SO_2, in order to prevent the formation and influence of gypsum, so that the more intrinsic dissolution behavior can be studied. Note that when using a strong acid to neutralize limestone with the same supply rate, there is a small difference between sulfuric acid and hydrochloric acid [28]. In this study, in order to prevent the adhesion of byproduct $CaSO_4$ on the limestone particles (which may strongly affect the measurement of particle size distribution), hydrochloric acid is used in the present study. Again we note that the present fundamental experimental study focuses on the effects of various parameters on the intrinsic characteristics of dissolution, including the source of limestone, particle size, pH, and temperature, and these parameters are varied in large ranges (which do not necessarily correspond to the real working conditions of WFGD,[1] thus the findings are not limited to WFGD and they are also applicable to many other processes involving limestone and acid solutions).

[1] In one of our previous studies [29] which experimentally involved limestone and dissolved SO_2 under working conditions that are more relevant to the WFGD industry, the useful process parameters for improving the efficiency of the WFGD process were explored.

The dissolution reaction occurs in a beaker, which is immersed in a water bath whose temperature is controlled at a desired level. Since the solid particle concentration has little influence on limestone reactivity [29], 1.2 g of limestone powder is added into 0.05 M $CaCl_2$ at the beginning of the experiment. A large amount of 0.1 M HCl is contained in the acid holding bottle, the supply rate of which toward the reaction beaker is adjusted by a pH controller (using a compound electrode dipped into the reaction solution to detect the pH value); in this way, a constant pH value can be kept in the reaction beaker. A mechanical stirrer provides a sufficiently fast stirring speed to keep the reactants and products mixed uniformly. The consumed quantity of HCl is recorded in-situ, from which the dissolution rate of limestone samples may be deduced. A pump circulates the liquid into the laser particle size analyzer, and the in-situ information of the size distribution of unreacted limestone particles is obtained. For different experiments, the testing conditions are as varied as following: temperature from 30 to 60 °C, and liquid pH value from 4.6 to 6.2.

2.2. Limestone samples

The limestone samples are from four different sources (Jiaochang, Liquan, Tanyu, Xinjiang), whose contents and physical properties are listed in Table 1. Each type of limestone is sieved to four batches of samples with different particle size distributions, which are measured by the laser particle size analyzer. The average particle diameter of each batch of sample is listed in Table 2. In the name of the sample, the first number indicates the source of limestone sample ("1" indicates Liquan, "2" indicates Tanyu, "3" indicates Jiaochang, and "4" indicates Xinjiang) and the second number indicates the different batches of particle size distributions (with "1" being the smallest and "4" the largest). From the optical microscopy (Fig. 2) it can be seen that the typical particles from limestone samples have a certain size distribution, and most particles are not spherical ("regular" or "ideal" shape).

2.3. Experimental conditions

Three groups of working conditions similar to that encountered in WFGD are examined, based on the reaction temperatures and system pH values: Group 1 (Table 3) with reaction temperature 50 °C and pH value 5.4, for 16 limestone samples (with different particle size distributions) from four different sources; Group 2 (Table 4) with reaction temperature 50 °C and pH value 4.6–6.2, for four limestone samples (with different particle size distributions) from four different sources; and Group 3 (Table 5) with reaction

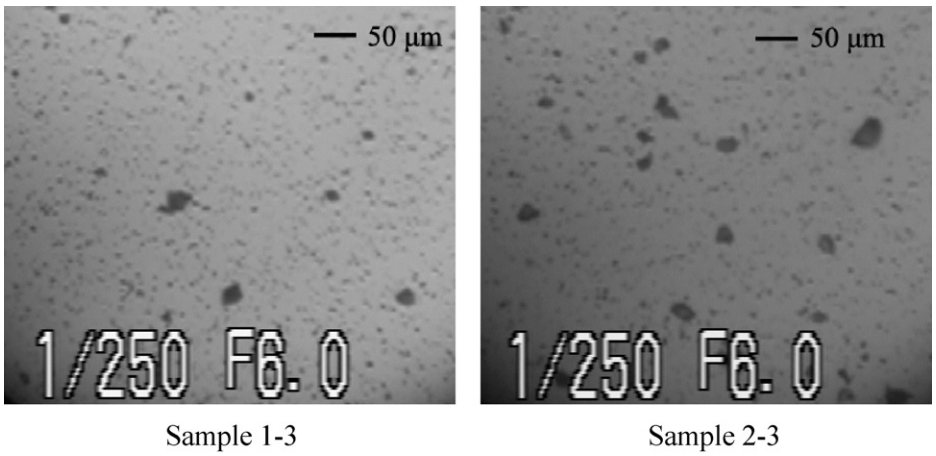

Fig. 2. Optical micrograph of limestone particles.

Table 3
Experimental conditions of Group 1.

Label	Conditions		
	pH value	T/°C	Samples
1-1-1	5.4	50	Sample 1-1
1-1-2			Sample 1-2
1-1-3			Sample 1-3
1-1-4			Sample 1-4
1-3-1	5.4	50	Sample 3-1
1-3-2			Sample 3-2
1-3-3			Sample 3-3
1-3-4			Sample 3-4
1-2-1	5.4	50	Sample 2-1
1-2-2			Sample 2-2
1-2-3			Sample 2-3
1-2-4			Sample 2-4
1-4-1	5.4	50	Sample 4-1
1-4-2			Sample 4-2
1-4-3			Sample 4-3
1-4-4			Sample 4-4

Table 4
Experimental conditions of Group 2.

Label	Conditions		
	pH value	T (°C)	Samples
2-1-1	4.6	50	Sample 1-3
2-1-2	5		
2-1-3	5.4		
2-1-4	5.8		
2-1-5	6.2		
2-3-1	4.6	50	Sample 3-3
2-3-2	5		
2-3-3	5.4		
2-3-4	5.8		
2-3-5	6.2		
2-2-1	4.6	50	Sample 2-3
2-2-2	5		
2-2-3	5.4		
2-2-4	5.8		
2-2-5	6.2		
2-4-1	4.6	50	Sample 4-3
2-4-2	5		
2-4-3	5.4		
2-4-4	5.8		
2-4-5	6.2		

temperature 30–60 °C and pH value 5.4, for four limestone samples (with different particle size distributions) from four different sources.

3. Experimental results and discussion

3.1. Dissolution characteristics

If a strong acid, for example, hydrochloric acid, is added to stirred limestone slurry, the dissolution of limestone follows the reaction:

$$CaCO_3 + 2H^+ \rightarrow Ca^{2+} + CO_2 + H_2O \quad (1)$$

Therefore, by measuring the consumed quantity of hydrochloric acid during the dissolution process, the mass of unreacted limestone samples can be obtained in-situ. On the other hand, by studying the in-situ particle size distribution of the unreacted limestone samples, the dissolution characteristics of different limestone samples under various testing conditions can be explored. Take the limestone samples 1-3, 2-3, 3-3, and 4-3 as illustrative examples, in Figs. 3–6 their dissolution characteristics are given under reacting pH value 5.4 and temperature 50 °C (experimental condition Group 1, Table 3). In these figures, (a) represents the mass of remaining limestone varying with dissolution time, (b) and (c) represent the particle size distribution at particular instants, during the earlier and later stages of the dissolution process, respectively.

Table 5
Experimental conditions of Group 3.

Label	Conditions		
	pH value	T (°C)	Samples
3-1-1	5.4	30	Sample 1-3
3-1-2		40	
3-1-3		50	
3-1-4		60	
3-3-1	5.4	30	Sample 3-3
3-3-2		40	
3-3-3		50	
3-3-4		60	
3-2-1	5.4	30	Sample 2-3
3-2-2		40	
3-2-3		50	
3-2-4		60	
3-4-1	5.4	30	Sample 4-3
3-4-2		40	
3-4-3		50	
3-4-4		60	

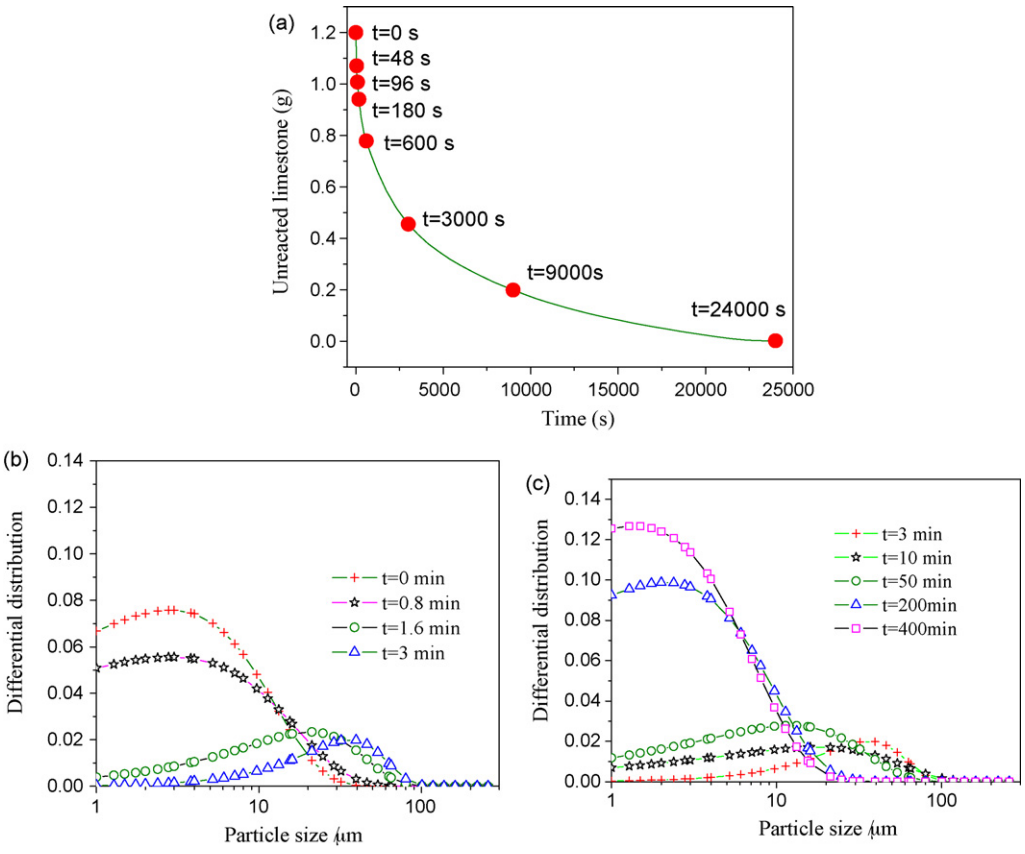

Fig. 3. Effect of particle size distributions during dissolution process: (a) the time evolution of the mass of unreacted limestone sample, (b) the differential distributions at 0, 48, 96 and 180 s during dissolution process and (c) the differential distributions at 180, 600, 3000, 9000 and 24,000 s during dissolution process of Liquan limestone 1-3 at 50 °C and pH 5.4.

While the overall trend is that the total mass of unreacted limestone decays exponentially with time, the variation of the particle size distribution is not monotonic. During the first 3 min of reaction, the wave crest of differential distribution moves toward the bigger particles, which means that the finer particles that have larger specific areas react and diminish at a higher rate. With the increased reaction time, the wave crest of differential distribution moves toward the smaller particles, indicating that the bigger particles dissolve and break into smaller ones. Therefore, the initial particle size distribution of the sample (e.g. ratio between finer and bigger particles) has a significant effect on the process of dissolution.

In order to quantitatively characterize the dissolution rate on a unit surface area of the limestone particles, the following estimation is carried out. Suppose the limestone particles with sizes between $[x_{i-1}, x_i]$ have an averaged relative mass fraction w_i (the density is ρ and the total mass of the sample is M). Assume all limestone particles are nonporous and spherical, the number of limestone particles within the interval $[x_{i-1}, x_i]$ can be estimated as:

$$n_i = \frac{6 \times w_i M}{\rho \pi \bar{x}_i^3} \tag{2}$$

where $\bar{x}_i = (x_{i-1} + x_i)/2$. The total particle number of the entire sample is the summation of n_i. The total surface area of the limestone sample is

$$A_S = \sum_{i=1}^{m} n_i s_i = 6 \times \sum_{i=1}^{m} \frac{w_i M \bar{x}_i}{\rho} \tag{3}$$

Combined with the limestone mass consumption rate dm/dt measured in experiment (e.g. Fig. 3(a)), the dissolution rate on unit surface area of limestone particle can be obtained as following:

$$\frac{dm}{dt \times A_S} = \frac{1}{6} \times \frac{dm}{dt} \times \frac{\rho}{\sum_{i=1}^{m} w_i M \bar{x}_i} \tag{4}$$

Based on the above calculations, Figs. 7–9 show the time evolution of the total number of unreacted limestone particles, $\sum_{i=1}^{m} n_i$, and dissolution rates on unit surface area, $dm/(dt \times A_S)$, for different limestone sources, different pH, and different temperatures, respectively. It can be observed that during the early stage of dissolution process, the total number of unreacted limestone particles decreases rapidly and the dissolution rate is much higher, which is controlled by surface reaction kinetics. In the later stage of dissolution process, the dissolution rate varies very slowly since it is mainly controlled by diffusion; meanwhile, the quantity of unreacted limestone particles may increase in some occasions – on one hand, the fluctuation of particle number may be expected since larger particles may break into smaller ones during the dissolution process (due to the porous structures of limestone particles), on the other hand, the error of Eq. (2) (and any error of the calculated limestone particle number in Figs. 7(a), 8(a), and 9(a)) may be resulted from the irregular shape (see Fig. 2) of limestone particles in practice.

3.2. Discussion

The experimental results indicate a significant effect of particle size on dissolution characteristics. Since the particle size distribution can be measured in practice, in order to quantitatively explain the particle size effect, the dissolution process of a single limestone particle needs to be described. Among the previous studies on the dissolution rate of limestone [21,25–27], the shrinking-core model is a fundamental approach to describe such a dissolution

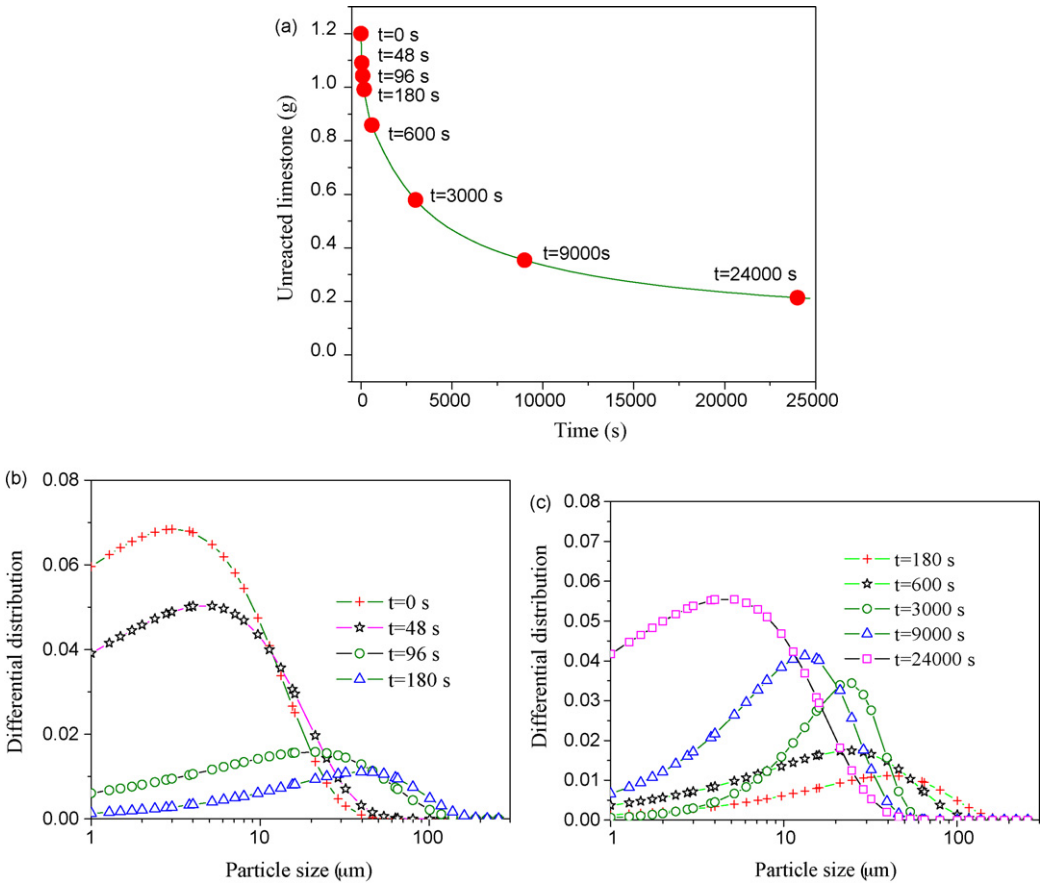

Fig. 4. Effect of particle size distributions during dissolution process: (a) the time evolution of the mass of unreacted limestone sample, (b) the differential distributions at 0, 48, 96 and 180 s during dissolution process and (c) the differential distributions at 180, 600, 3000, 9000 and 24,000 s during dissolution process of Tanyu limestone 2-3 at 50 °C and pH 5.4.

process. Assuming the limestone particle is nonporous and spherical, the dissolution rate per unit surface area of the particle can be expressed by [26,27]:

$$-\rho_m \frac{dr_p}{dt} = k(C_{H^+} - C_S^*) \tag{5}$$

where ρ_m is the molar concentration of $CaCO_3$ and $MgCO_3$ in the limestone sample, kmol/m^3; r_p is the radius of limestone particle, m; k is a dissolution rate constant, m/s; t is reaction time, s; C_{H^+} is the concentration of H^+ in reaction solution, kmol/m^3; C_S^* is the concentration of H^+ at the surface of limestone particle, kmol/m^3. The mass transfer coefficient in the stagnant fluid (i.e. the Sherwood number) is given by:

$$Sh = \frac{k \times 2r_p}{D} = 2 \tag{6}$$

From Eqs. (5) and (6):

$$\frac{dr_p}{dt} = -\frac{D}{r_p \rho_m}(C_{H^+} - C_S^*) \tag{7}$$

In the dissolution process of limestone in acidic solution, C_{H^+} is much greater than C_S^* [26], and thus C_S^* can be neglected in Eq. (7). In order to obtain the evolution of limestone particle size, the expression of the diffusion coefficient D needs to be identified. However, it is often difficult to define D during liquid–solid reaction, which is affected by many factors. According to the dissolution curve (such as Figs. 3(a)–6(a)), the final empirical equation should be in an exponential form, therefore, we define a synthesized diffusion coefficient D' to replace D:

$$D' = k_D r_p^2 \tag{8}$$

k_D is diffusion velocity coefficient, s^{-1}. Substitute Eq. (8) into Eq. (7) and integrate:

$$r_p = r_0 \times \exp\left(-\frac{1}{k_D}\frac{C_{H^+}}{\rho_m}t\right) \tag{9}$$

In the above, r_0 is the initial radius of limestone particle before dissolution, m. The dissolution ratio of a single limestone particle

Table 6
Coefficients of different limestone used in the model.

Habitat	Coefficient					
	k_1	k_2	K	A	B	C
Liquan limestone	423.55	3.4158	2.5588	0.67117	−10.457	2.0353
Tanyu limestone	756.51	1.8960	2.2241	0.42380	−6.3307	0.46727
Jiaochang limestone	388.39	0.25910	144.79	0.92953	−9.2530	1.1369
Xinjiang limestone	497.98	0.22994	48.113	0.77716	−13.116	0.82735

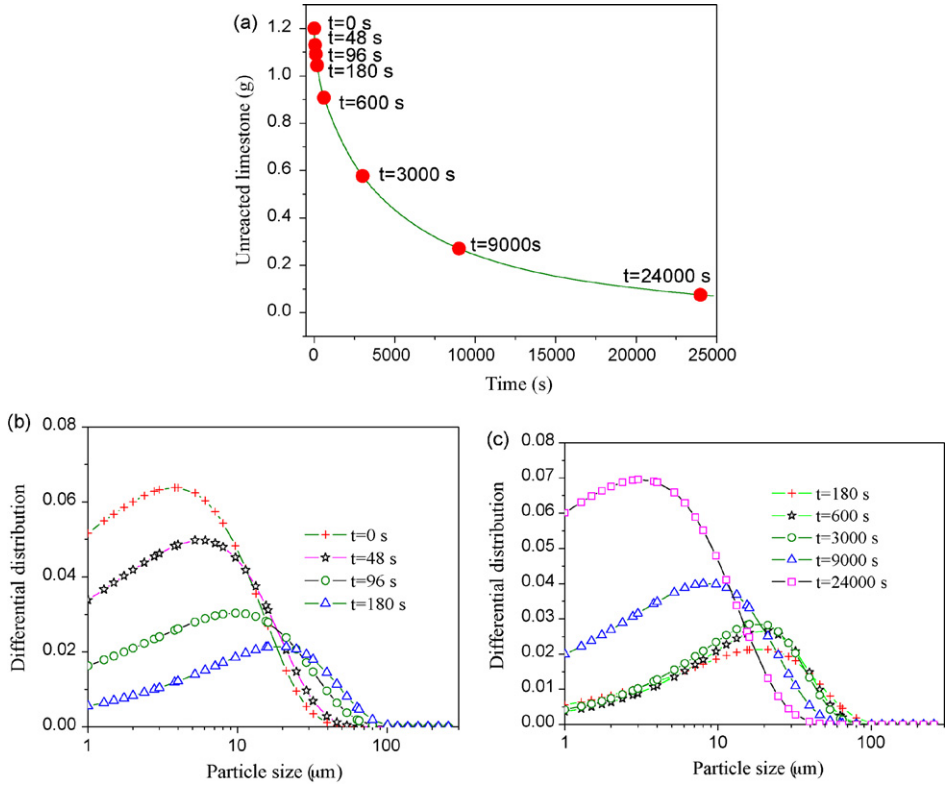

Fig. 5. Effect of particle size distributions during dissolution process: (a) the time evolution of the mass of unreacted limestone sample, (b) the differential distributions at 0, 48, 96 and 180 s during dissolution process and (c) the differential distributions at 180, 600, 3000, 9000 and 24,000 s during dissolution process of Jiaochang limestone 3-3 at 50 °C and pH 5.4.

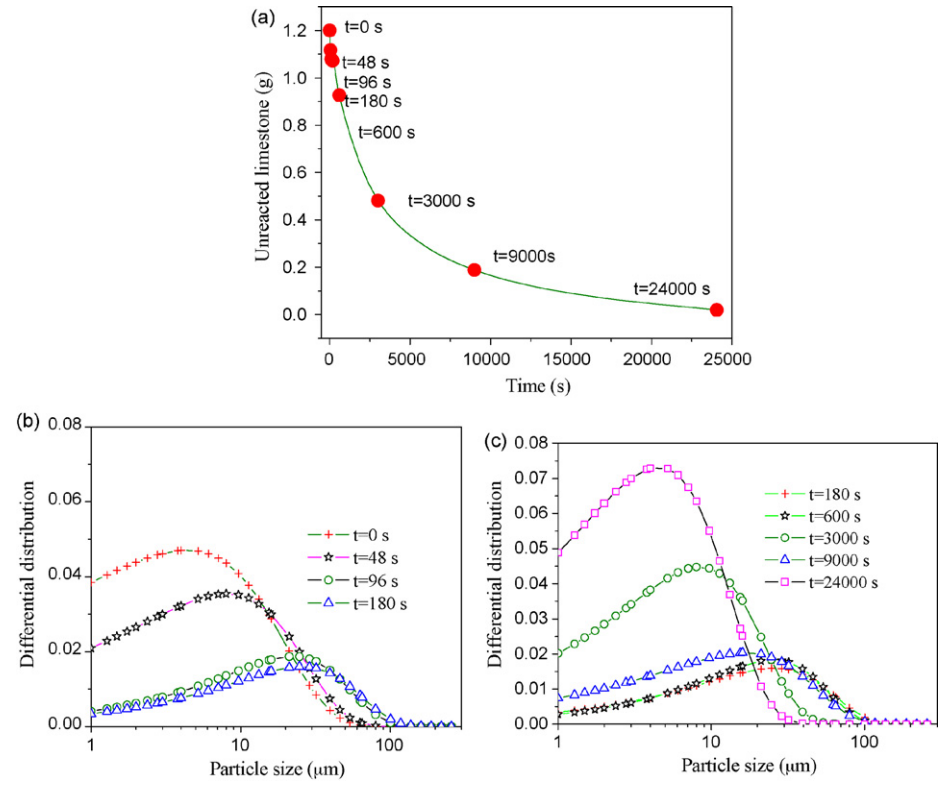

Fig. 6. Effect of particle size distributions during dissolution process: (a) the time evolution of the mass of unreacted limestone sample, (b) the differential distributions at 0, 48, 96 and 180 s during dissolution process and (c) the differential distributions at 180, 600, 3000, 9000 and 24,000 s during dissolution process of Xinjiang limestone 4-3 at 50 °C and pH 5.4.

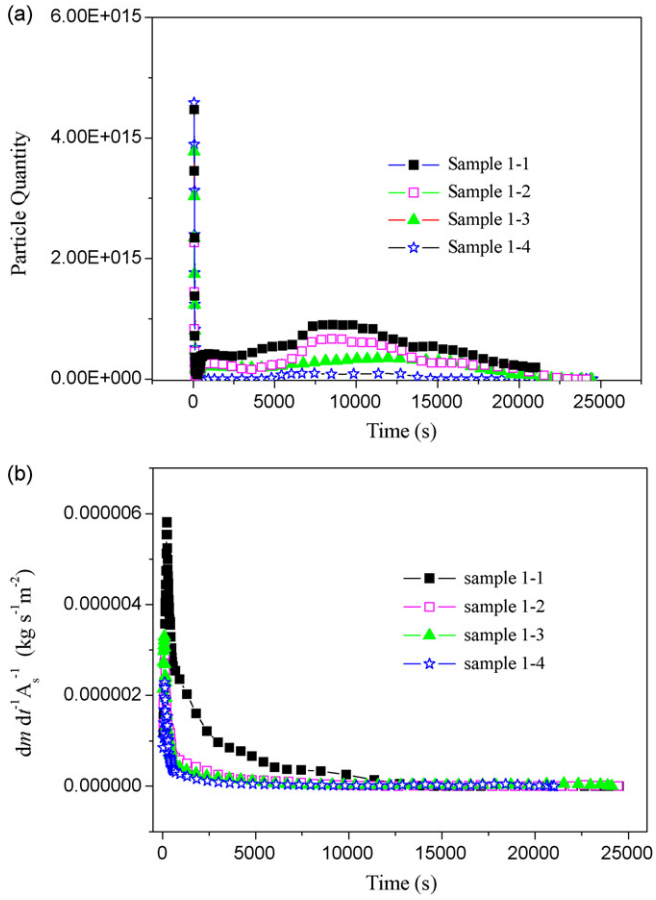

Fig. 7. Dissolution characteristics: (a) the time evolution of the total number of unreacted limestone particles and (b) the dissolution rate on unit surface area of Liquan limestone (different samples 1-1–1-4) at 50 °C and pH 5.4.

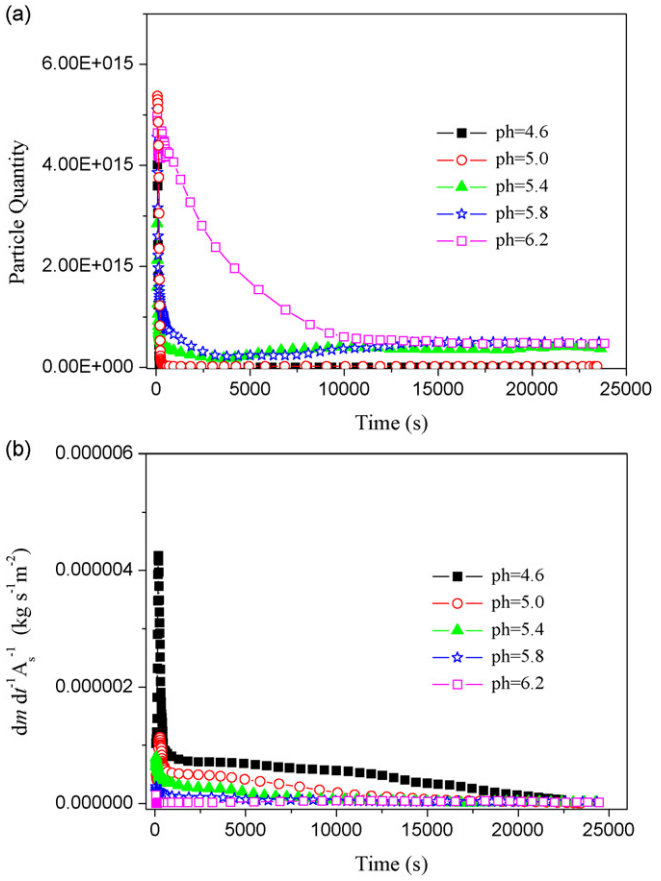

Fig. 8. Dissolution characteristics: (a) the time evolution of the total number of unreacted limestone particles and (b) the dissolution rate on unit surface area of Jiaochang limestone 3-3 at 50 °C and pH varying between 4.6 and 6.2.

can be represented as:

$$y = 1 - \left(\frac{r_p}{r_0}\right)^3 = 1 - \left(\exp\left(-\frac{1}{k_D}\frac{C_{H^+}}{\rho_m}t\right)\right)^3 \quad (10)$$

Given the dissolution characteristics measured from our experiment, it is anticipated that k_D is large during the early stage and becomes smaller during the later stage of the dissolution process. We assume that the evolution of k_D follows the smooth function:

$$\frac{1}{k_D} = (\tau_2 - \tau_1)\left(1 - \exp\left(-\left(\frac{r_0 - r_p}{r_0}K'\right)^{n'}\right)\right) + \tau_1 \quad (11)$$

Here, τ_1 and τ_2 are two constants governing the value range of k_D, n' and K' are two constants governing the gradient and transition of the evolution of k_D. In order to describe the dissolution characteristics of different limestone samples under various experimental conditions obtained above, two reaction rate constants (k_1, k_2) are introduced into the equation to reflect the two factors of surface reaction kinetics and diffusion. An empirical equation describing the dissolution process of a single particle can be obtained as (where we assume that the effects of temperature, pH value and initial particle size can be expressed as power-law functions):

$$\frac{dr_p}{dt} = -\frac{1}{((1/k_1) + (1/k_2) \times (1 - \exp(K((r_0 - r_p)/r_0)(C_{H^+}/C^0)^A(T/T^0)^B(\overline{d_0}/d^0)^C)))}\frac{C_{H^+}}{\rho_m}r_p \quad (12)$$

Here, T is the reaction temperature, K; k_1 and k_2 are reaction rate constants, s^{-1}, which depend on the type of limestone; $\overline{d_0}$ is the initial average grain diameter of sample, m; $C^0 = 1\ kmol/m^3$, $T^0 = 273\ K$, and $d^0 = 1\ m$ are reference values for normalization; A, B, and C are empirical coefficients that represent the effects of pH value, temperature, and initial particle size, respectively. K is another empirical coefficient reflecting the effect of particle shape. The empirical coefficients are listed in Table 6.

Suppose y_i is the average relative dissolution ratio for particles within the interval $[x_{i-1}, x_i]$. With the initial particle size distribution, from Eq. (12) one can predict the mass consumption rate of all limestone particles:

$$Y = \sum_{i=1}^{n}(w_i \times (1 - y_i)) = \sum_{i=1}^{n}\left(w_i \times \left(1 - \left(\frac{r_{pi}}{r_{0i}}\right)^3\right)\right) \quad (13)$$

where $r_{0i} = \bar{x}_i/2$. Figs. 10–12 show the time-dependence of dissolution ratio of several representative limestone samples, where the testing conditions are varied. Similar results hold for other samples at other testing conditions. The solid curves in these figures show the prediction by Eq. (12), which are in good agreement with the experimental data. Both the experimental data and Eq. (12) indicate that, for a given type of limestone, the dissolution reaction rate is higher if the average particle size is smaller (see Fig. 11), or when temperature is higher (see Fig. 13), or when pH is lower (see Fig. 12). On the other hand, the average particle sizes of samples 1-1, 1-2, 3-3 and 4-2 are close to 18 mm, however they have different molar contents of CaO and MgO: the molar content in sample 3-3 > sample 1-2 > sample 2-2 > sample 4-2. Fig. 10 indicates that the chemical composition has some influence on the dissolution

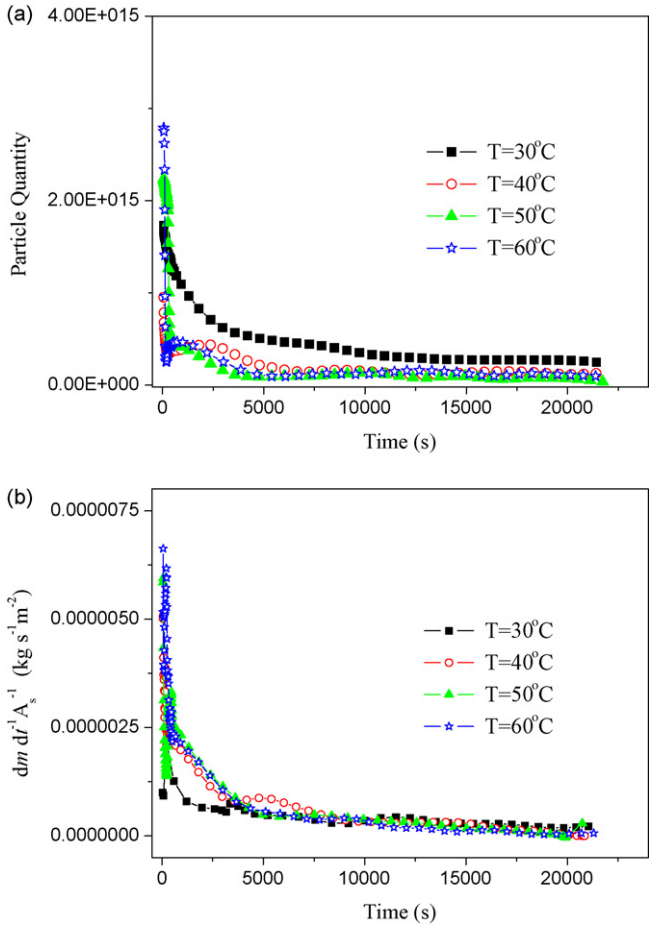

Fig. 9. Dissolution characteristics: (a) the time evolution of the total number of unreacted limestone particles and (b) the dissolution rate on unit surface area of Xinjiang limestone 4-3 at pH 5.4 and as the temperature varies from 30 to 60 °C.

rate, in addition to and may be coupled with the effects of the limestone source and particle size distribution. Overall, the empirical equation (12) is generic and it can well describe the dissolution rate for a large range of particle size distribution, ambient temperature, and pH value. For limestone samples from the same source, the reaction rate constants (k_1, k_2) and empirical coefficients (K,

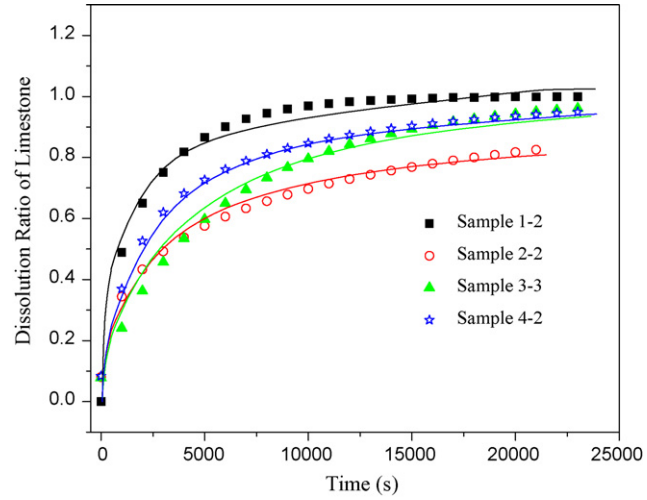

Fig. 10. Dissolution rates at 50 °C and pH 5.4 for different limestone samples 1-2, 2-2, 3-3 and 4-2; lines are predictions from the model.

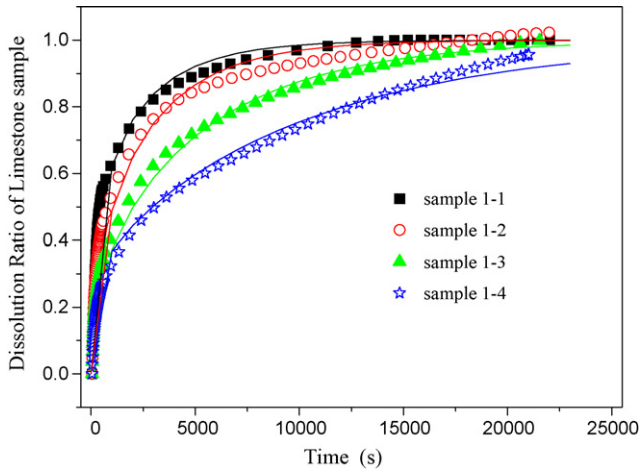

Fig. 11. Dissolution rates at 50 °C and pH 5.4 for different limestone samples 1-1–1-4; lines are predictions from the model.

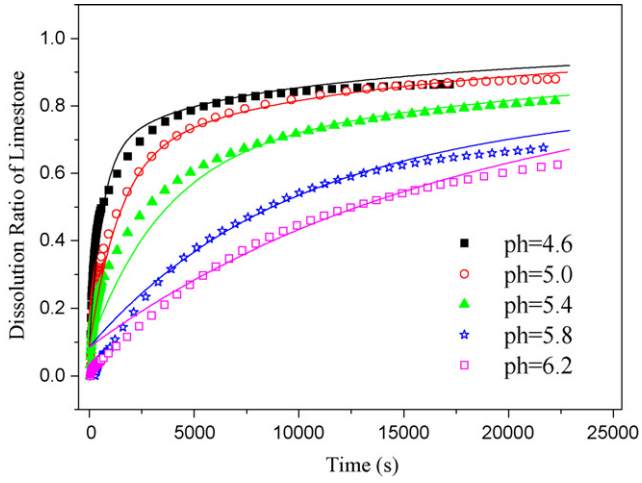

Fig. 12. Dissolution ratio of limestone at 50 °C and different pH values 4.6, 5.0, 5.4, 5.8, 6.2 for limestone sample 2-3; lines are predictions from the model.

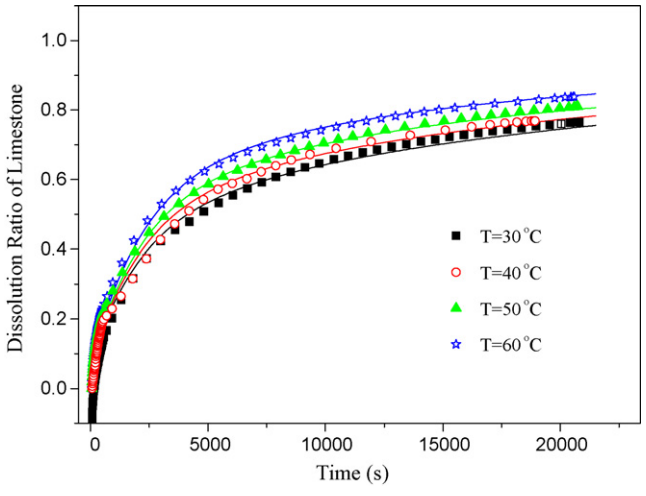

Fig. 13. Dissolution ratios of limestone at different temperatures 30, 40, 50, 60 °C, with pH 5.4 for limestone sample 3-3.

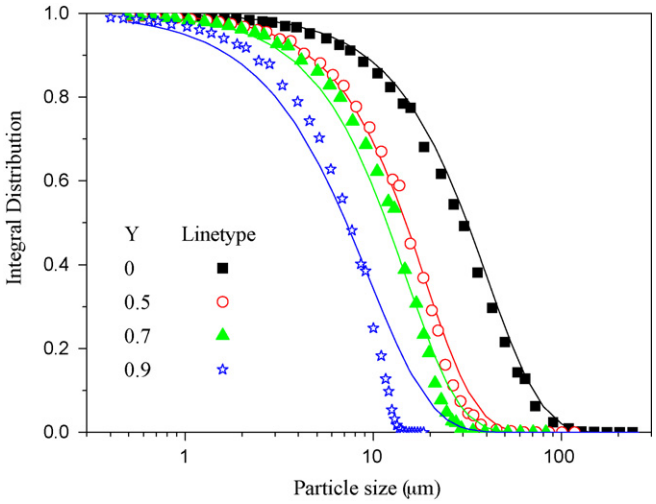

Fig. 14. Particle size distributions of unreacted limestone for four different dissolution ratios (Y) in a dissolution process, for Xinjiang limestone 4-3 at 50 °C and pH 5.4.

A, B, C) in Eq. (12) are invariant constants; for different limestone sources they take different values.

Another verification of Eq. (12) is shown in Fig. 14, where from the initial particle size distribution of limestone sample and Eq. (12), the particle size distributions of unreacted limestone at any instant during the dissolution process can be predicted. The predictions (solid curves) of Xinjiang sample 4-3 (at 50 °C and pH 5.4) agree well with experimental observation; the error with respect to measurement gets larger near the end of dissolution process, since only few limestone particles remain. Similar good agreements are found in other limestone samples at other conditions.

4. Conclusion

In this experimental study, in-situ information of limestone dissolution is obtained for different limestone sources, initial particle size distributions, temperatures, and pH values, from which important insights of liquid–solid particle reaction is obtained. It is found that the dissolution rate (per unit surface area of limestone particle) is higher when the average particle size is smaller, the temperature is higher, and pH value is lower. The chemical composition also has some influence on the dissolution rate. Based on a shrinking-core model, an empirical equation is proposed which can correlate the dissolution rate of a single particle with particle size and working conditions. The predictions of the empirical equation, including the effects of particle size, pH value and temperature, agree well with experimental measurements. The results may help to design the FGD process more efficiently.

Acknowledgements

BS and QZ are supported in part by the National Natural Science Foundation of China (50928601) and the National Basic Research Program of China (2005CB221206). BS is also supported by the State 973 Program of China (2007CB210102), China Scholarship Council, and the Shanghai Science and Technology Commission, Shanghai China (No. 08DZ1204202). XC is supported by the National Science Foundation (CMMI-0643726), the National Natural Science Foundation of China (50928601), and the National Research Foundation of Korea (R32-2008-000-20042-0).

References

[1] H.G. Nygaard, S. Kiil, J.E. Johnsson, Full-scale measurements of SO_2 gas phase concentrations and slurry compositions in a wet flue gas desulphurisation spray absorber, Fuel 83 (2004) 1151–1164.
[2] J. Kaminski, Technologies and costs of SO_2-emissions reduction for the energy sector, Applied Energy 75 (2003) 165–172.
[3] P.S. Nolan, K.E. Redinger, G.T. Amrhein, G.A. Kudlac, Demonstration of additive use for enhanced mercury emissions control in wet FGD systems, Fuel Processing Technology 85 (2004) 587–600.
[4] D.S. Jin, B.R. Deshwal, Y.S. Park, H.K. Lee, Simultaneous removal of SO_2 and NO by wet scrubbing using aqueous chlorine dioxide solution, Journal of Hazardous Materials 135 (2006) 412–417.
[5] R.V. Bravo, C.F. Camacho, V.M. Moya, A.I. Garcia, Desulphurization of SO_2-NO_2 mixtures by limestone slurry, Chemical Engineering Science 57 (2002) 2047–2058.
[6] J.W. Morse, R.S. Arvidson, The dissolution kinetics of major sedimentary carbonate minerals, Earth Science Reviews 58 (2002) 51–84.
[7] Z.O. Siagi, M. Mbarawa, Dissolution rate of South African calcium-based materials at constant pH, Journal of Hazardous Materials 163 (2007) 678–682.
[8] C. Hosten, M. Gulsun, Reactivity of limestone from different sources in Turkey, Minerals Engineering 17 (2004) 97–99.
[9] A. Stergarsek, M. Gerbec, R. Kocjančič, P. Frkal, Modelling and experimental measurements of limestone dissolution under enhanced wet limestone FGD process conditions, Acta Chimica Slovenska 46 (1999) 323–333.
[10] L. Plan, Factors controlling carbonate dissolution rates quantified in a field test in the Austrian Alps, Geomorphology 68 (2005) 201–212.
[11] S. Aydoğan, M. Erdemoğlu, G. Uçar, A. Aras, Kinetics of Galena dissolution in nitric acid solutions with hydrogen peroxide, Hydrometallurgy 88 (2007) 52–57.
[12] D.K. Gledhill, J.W. Morse, Calcite dissolution kinetics in Na–Ca–Mg–Cl brines, Geochimica et Cosmochimica Acta 70 (2006) 5802–5813.
[13] C. Noiriel, L. Luquot, B. Madé, L. Raimbault, P. Gouze, J.v.d. Lee, Changes in reactive surface area during limestone dissolution: An experimental and modelling study, Chemical Geology 265 (2009) 160–170.
[14] R.A. Berner, J.W. Morse, Dissolution kinetics of calcium carbonate in seawater: IV. Theory of calcite dissolution, American Journal of Science 274 (1974) 108–134.
[15] D. Buhman, W. Dreybrot, The kinetics of calcite dissolution and precipitation in geologically relevant situations of karst areas: 1. Open system, Chemical Geology 48 (1985) 189–211.
[16] D. Buhman, W. Dreybrot, The kinetics of calcite dissolution and precipitation in geologically relevant situations of karst areas: 2. Closed system, Chemical Geology 53 (1985) 109–124.
[17] L.N. Plummer, T.M.L. Wigley, D.L. Parkhurst, The kinetics of calcite dissolution in CO_2–water systems at 5 to 60 °C and 0.0 to 1.0 atm CO_2, American Journal of Science 278 (1978) 179–216.
[18] L.N. Plummer, D.L. Parkhurst, T.M.L. Wigley, A critical review of the kinetics of calcite dissolution and precipitation, ACS Symposium Series 93 (1979) 537–573.
[19] H. Rutto, Z. Siagi, M. Mbarawa, Effect of ammonium compounds on dissolution rate of South African calcium-based material, Journal of Hazardous Materials 168 (2009) 1532–1536.
[20] T. Takashina, S. Honjo, N. Ukawa, K. Iwashita, Effect of ammonium concentration on SO_2 absorption in a wet limestone gypsum FGD process, The Society of Chemical Engineers 35 (2002) 197–204.
[21] P.K. Chan, G.T. Rochelle, Limestone dissolution: effects of pH, CO_2 and buffers modeled by MAA transfer, ACS Symposium Series 97 (1982) 75–97.
[22] A.J. Toprac, G.T. Rochelle, Limestone dissolution in stack gas desulfurization, Environmental Progress 1 (1982) 52–58.
[23] C.L. Gage, G.T. Rochelle, Limestone dissolution in flue gas scrubbing: effect of sulfite, Journal of Air Waste Management 42 (1992) 926–935.
[24] N. Ukawa, T. Takashina, N. Shinoda, Effects of particle size distribution on limestone dissolution in wet FGD process applications, Environmental Progress 12 (1993) 238–242.
[25] J. Ahlbeck, T. Engman, M. Vihma, A method for measuring the reactivity of absorbents for wet flue-gas desulfurization, Chemical Engineering Science 48 (1993) 3479–3484.
[26] J. Ahlbeck, T. Engman, M. Vihma, Measuring the reactivity of limestone for wet flue-gas desulfurization, Chemical Engineering Science 50 (1995) 1081–1089.
[27] S.M. Shih, J.P. Lin, G.Y. Shiau, Dissolution rates of limestones of different sources, Journal of Hazardous Materials B79 (2000) 159–171.
[28] B. Sun, Q.L. Zhou, Z.H. Shi, Experimental study on limestone dissolution in acid solution, Challenges of Power Engineering and Environment (2007) 773–777.
[29] Z.H. Shi, Investigation on characteristics of limestone dissolution in acid solution, Ph.D. Thesis, Xi'an Jiaotong University (2004).